

Sergei Gepshtein · Michael Kubovy

## Stability and change in perception: spatial organization in temporal context

Received: 31 October 2003 / Accepted: 29 June 2004 / Published online: 23 October 2004  
© Springer-Verlag 2004

**Abstract** Perceptual multistability has often been explained using the concepts of adaptation and hysteresis. In this paper we show that effects that would typically be accounted for by adaptation and hysteresis can be explained without assuming the existence of dedicated mechanisms for adaptation and hysteresis. Instead, our data suggest that perceptual multistability reveals lasting states of the visual system rather than changes in the system caused by stimulation. We presented observers with two successive multistable stimuli and found that the probability that they saw the favored organization in the first stimulus was inversely related to the probability that they saw the same organization in the second. This pattern of negative contingency is orientation-tuned and occurs no matter whether the observer had or had not seen the favored organization in the first stimulus. This adaptation-like effect of negative contingency combines multiplicatively with a hysteresis-like effect that increases the likelihood of the just-perceived organization. Both effects are consistent with a probabilistic model in which perception depends on an orientation-tuned intrinsic bias that slowly (and stochastically) changes its orientation tuning over time.

**Keywords** Vision · Perceptual organization · Multistability · Adaptation · Hysteresis · Bias · Orientation tuning · Sensory integration

### Introduction

We usually perceive a stable visual world with no hint of ambiguity of visual stimulation; but because such ambiguity exists the brain must often make perceptual decisions: it must select among the perceptual alternatives that are consistent with the optical stimulation (von Helmholtz 1867/1962; Ittelson 1952; Rock 1975; Marr 1982). Normally, these decisions are hidden from awareness; they are “unobservable” (or “private”). One way to make the process of perceptual selection observable is to look at ambiguous—or “multistable”—figures (Julesz and Chang 1976; Kruse and Stadler 1995; Kanizsa and Luccio 1995).

Thanks to studies of animals viewing multistable figures (reviewed in Leopold and Logothetis 1999 and Blake and Logothetis 2002) we understand some of the mechanisms responsible for perceptual selection. Several interpretations of a multistable stimulus are represented in the visual cortical activity concurrently, even though only one of the alternatives is perceived at a time. How can perceptual experience be stable and continuous in the presence of other interpretations? To answer this question, we must understand the interplay of two counteracting temporal tendencies in the perception of multistable figures: *hysteresis* and *adaptation*. Hysteresis increases the likelihood of the current percept in the next instant; adaptation decreases it.

### Hysteresis

This tendency resembles a memory-like phenomenon in a system whose state depends on its history. If the perception of an ambiguous stimulus persists even after the stimulus has been changed to the point where its geometry favors an alternative interpretation, the perceptual system is said to show hysteresis with respect to this type of ambiguous stimulus (Fender and Julesz 1967; Williams et al. 1986; Hock et al. 1993; Kruse and Stadler 1995).

---

This work was supported by NEI Grant R01 EY 12926

S. Gepshtein (✉)  
Vision Science, University of California at Berkeley,  
360 Minor Hall,  
Berkeley, CA 94720-2020, USA  
e-mail: sergeg@uclink.berkeley.edu

M. Kubovy (✉)  
Department of Psychology, University of Virginia,  
P.O. Box 400400 Charlottesville, VA 22904-4400, USA  
e-mail: kubovy@virginia.edu

## Adaptation

This tendency resembles the common perceptual process in which prolonged exposure to a stimulus makes the system less sensitive to the parameters of the stimulus (e.g., Hochberg 1950; Kruse et al. 1986). Following Köhler and Wallach (1994) and Carlson (1953), a common explanation of the reduced sensitivity is neural fatigue (reviewed in Rock 1975, pp. 265–270; but see Barlow 1990 for a different explanation).

Because these two tendencies oppose each other, they may cancel out and obscure their individual contributions and the rules of their combination. In this study we describe a method that allows us to separate the two effects and determine how they combine.

Our method is a development of the technique introduced by Hock et al. (1996), who used bistable motion quartets (von Schiller 1933; Fig. 1). These are apparent motion displays that allow two interpretations, which in Fig. 1 are horizontal motion and vertical motion. Motion is seen more often between dots separated by the shorter spatial distance. Let  $d_h$  and  $d_v$  stand for horizontal and vertical inter-dot distances, respectively. By manipulating the aspect ratio,  $R=d_v/d_h$ , one can vary the probabilities of the two alternative motion directions, as shown in Fig. 1.

Hock et al. 1996 showed observers two motion quartets— $M_1$  (*adapting*) and  $M_2$  (*test*)<sup>1</sup>—in rapid succession in order to discover whether the visual system is adapted by the unperceived interpretations of  $M_1$ . They manipulated the aspect ratio  $R_1$  of quartet  $M_1$ , and kept the aspect ratio of  $M_2$  constant and unbiased:  $R_2=1.0$ . They obtained the probabilities of the observers' responses to  $M_1$  and  $M_2$  and asked how  $R_1$  affects the perception of  $M_2$  rather than asking how the *perception* of  $M_1$  ( $m_1$ ), affects the perception of  $M_2$  ( $m_2$ ). This question dictated the design of the experiment: they considered only those trials in which *vertical* motion was perceived during the adapting phase,  $m_1=\downarrow$ . (In other words, the authors held the observer's percept of  $M_1$  constant.) The dependent variable was the probability of *horizontal* motion during the test phase,  $p(m_2=\leftrightarrow)$ . The results were clear. They found that the conditional probability of reporting  $m_2=\leftrightarrow$  after

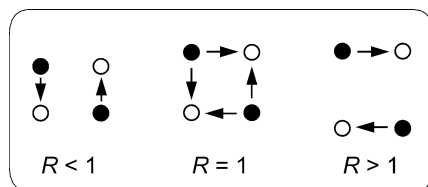


**Fig. 1** Motion quartets. Two pairs of identical dots (shown here as *filled and open circles*) are presented in alternation in the opposite corners of a rectangle. When the quartet aspect ratio  $R$  is equal to one, perception readily alternates between the two directions of motion—vertical and horizontal. The likelihood of these two percepts varies with  $R$ .

<sup>1</sup>We describe the experiments of Hock et al. (1996) using a convention different from theirs.

seeing  $m_1=\downarrow$ ,  $p(m_2=\leftrightarrow|m_1=\downarrow)$  was a decreasing function of  $R_1$ . They interpreted their results as evidence of adaptation of the visual system by a representation of  $M_1$  that was not experienced but whose existence left a trace in the system that affected the perception of  $M_2$ . They reasoned that increasing  $R_1$  led to a greater strength of the (unperceived) representation of horizontal motion, which in turn caused a greater adaptation to horizontal motion and reduced the likelihood of this motion in  $M_2$ .

We too study perceptual selection, but we use static rather than dynamic multistable stimuli. We generalize the method of Hock et al. (1996) such that we can also measure percept-percept correlations. This allows us to observe the balance between the counteracting trends in perception of multistable figures; we find that their effects combine multiplicatively. We also find that the interactions between successive perceptual organizations are orientation tuned. The results suggest a hypothesis that does not require adaptation and hysteresis as causal factors in perceptual selection. According to this hypothesis, the temporal contingencies between successive perceptual organizations occur because of lasting states of the visual system and not because the preceding stimulus changes (e.g., adapts) the system such as to affect the perception of succeeding stimuli.

---

## Experiment 1

In this experiment, we presented observers with a succession of two multistable dot lattices— $L_1$  and  $L_2$ —and recorded their perception of each lattice.

### Method

#### Observers

Five observers participated in experiment 1: one of the authors and four undergraduate students who did not know the purpose of the experiment. All the observers had normal or corrected-to-normal vision.

#### Stimuli

Our  $L_1$  stimuli were *rectangular* dot lattices (Fig. 2). (For the nomenclature of dot lattices, see Kubovy 1994.) The lattices were presented at random orientations by aligning one of the principal organizations of  $L_1$  with an axis of a randomly oriented system of Cartesian coordinates, whose origin was at the center of a circular aperture (as shown in Fig. 2). We will refer to this axis as  $0^\circ$ . Observers are most likely to see such a lattice as a collection of strips parallel to  $0^\circ$  or  $90^\circ$ . (The randomly chosen  $0^\circ$  orientation was the same for both successive lattices.)

The organization of  $L_1$  is controlled by its aspect ratio  $R_1=d_{90}/d_0$ , where  $d_0$  and  $d_{90}$  represent the inter-dot distances along the orientations parallel to  $0^\circ$  and  $90^\circ$ ,

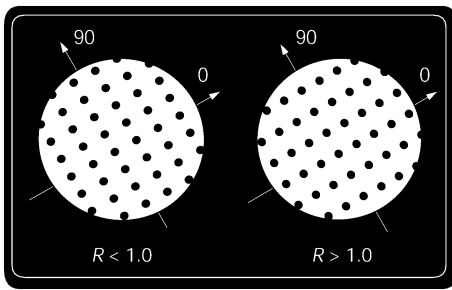


**Fig. 2** Two rectangular dot lattices in the rotating system of Cartesian coordinates (not to scale). *Left* when the aspect ratio is  $R=d_{90}/d_0 < 1.0$  we tend to see the lattice organized parallel to  $90^\circ$  (notated as  $l \rightarrow 90$ ). *Right* when the aspect ratio is  $R > 1.0$  we tend to see it organized parallel to  $0^\circ$  ( $l \rightarrow 0$ ).

respectively (Fig. 2). We will notate the percept of a lattice  $L_i$  parallel to an orientation  $\xi$  as:

$$l_i \rightarrow \xi.$$

For example, we will write the two most likely percepts of  $L_1$  as  $l_1 \rightarrow 0$  and  $l_1 \rightarrow 90$ . Our  $L_2$  stimuli were hexagonal dot lattices (Fig. 3), for which the three most likely perceptual organizations were parallel to  $0^\circ$ ,  $60^\circ$ , and  $120^\circ$ . These percepts are approximately equiprobable and exhaustive, i.e.,

$$p(l_2 \rightarrow 0) \approx p(l_2 \rightarrow 60) \approx p(l_2 \rightarrow 120) \approx 1/3.$$

We used hexagonal lattices as  $L_2$  because they are the most unstable dot lattices (Kubovy and Wagemans 1995) and are therefore most sensitive to imbalances in the mechanisms underlying perceptual grouping.

Dot diameter in  $L_1$ ,  $L_2$ , and the mask was 0.16 degrees of visual angle (dva). At  $R_1=1.0$ , the inter-dot distance was about 1 dva. To preserve the scale of lattices with other values of  $R_1$ , the inter-dot distances were varied so that their product,  $d_0 \times d_{90}$ , was invariant. For example,

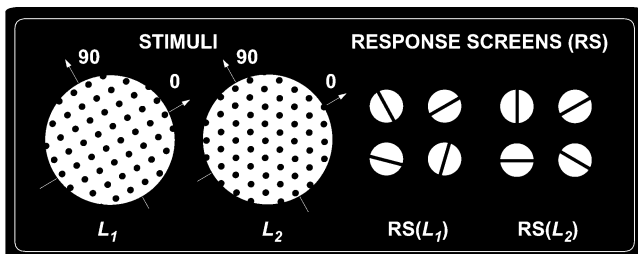


**Fig. 3** *Top panel* the two successive lattices—rectangular  $L_1$  and hexagonal  $L_2$ —and the two corresponding response screens. The fixation mark and the mask are not shown. *Bottom panel* the trial time line. The *dashed segments* represent durations under the observer's control.

with  $R_1=1.3$  the inter-dot distances were:  $d_0=0.88$  dva and  $d_{90}=1.14$  dva.

### Procedure

Each trial consisted of six successive screens (Fig. 3): fixation, lattices  $L_1$  and  $L_2$ , two response screens (one to report  $l_1$ , the other to report  $l_2$ ) and mask. Four of these—fixation,  $L_1$ ,  $L_2$  and mask—were presented on the background of a white circular aperture in a black field, subtending 11.5 dva. The fixation consisted of a dot in the center of the aperture. The mask consisted of a sequence of randomly positioned black dots, whose locations were updated at 60 Hz.

On each trial, lattices  $L_1$  and  $L_2$  were aligned with the  $0^\circ$  axis, which was randomly oriented (with  $1^\circ$  resolution) to minimize the propagation of perceptual bias between the trials.

Observers were asked to report the perceptual organization of  $L_1$  and  $L_2$  by clicking on icons in the corresponding successive response screens. Each response screen consisted of four icons, each containing a line parallel to one of the possible organizations in the corresponding dot lattice (Fig. 3).

Each observer contributed 120 trials to each of the five values of  $R_1$ .

### Results

We plot the results on a logit scale, where

$$\text{logit}[p(l_1 \rightarrow 0)] = \ln \frac{p(l_1 \rightarrow 0)}{p(l_1 \rightarrow 90)}, \quad (1)$$

and

$$\text{logit}[p(l_2 \rightarrow 0)] = \ln \frac{p(l_2 \rightarrow 0)}{\frac{p(l_2 \rightarrow 60) + p(l_2 \rightarrow 120)}{2}}. \quad (2)$$

We averaged the data across observers and then computed  $\text{logit}[p(l_1 \rightarrow 0)]$  to overcome floor effects at high aspect ratios.

In the responses to  $L_1$ , we found that  $\text{logit}[p(l_1 \rightarrow 0)]$  increases as a linear function of  $R_1$  (Fig. 4a). These results replicate the results in previous studies of perceptual grouping (e.g., Kubovy et al. 1998) and thus serve as a control.

In the rest of this paper we adopt the common convention in which persistence of a percept is described as “hysteresis.” We will refer to the negative contingency between the successive percepts as a function of  $R_1$  as “effect of  $R_1$ .”

To study the effect of perception of  $L_1$  on the perception of  $L_2$ , we separate the trials on which  $l_1 \rightarrow 0$  responses occurred from trials on which  $l_1 \rightarrow 90$  responses occurred.

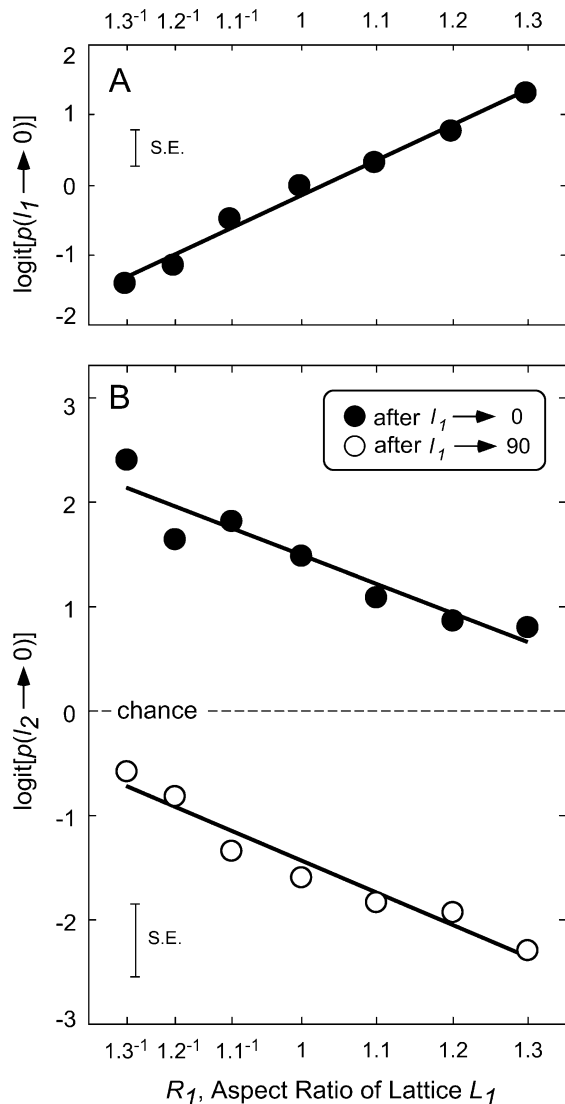


**Fig. 4** Results of experiment 1. **a** Responses to  $L_1$ . The data are well described by a linear model ( $R^2=0.987$ ). **b** Responses to  $L_2$ , conditionalized by the percepts of  $L_1$ . The label “after  $l_1 \rightarrow 0$ ” refers to events [ $l_2 \rightarrow 0 | l_1 \rightarrow 0$ ]. The label “after  $l_1 \rightarrow 90$ ” refers to events [ $l_2 \rightarrow 0 | l_1 \rightarrow 90$ ]. The variability in the two sets of data is well explained by a linear model (multiple regression  $R^2=0.985$ ).

By doing so we isolate the effect of perceptual hysteresis. Because hysteresis is a tendency to perceive the same organization in  $L_2$  as in  $L_1$ , we expect to find a higher likelihood of  $l_2 \rightarrow 0$  after  $l_1 \rightarrow 0$  than after  $l_1 \rightarrow 90$ . Indeed, we find that  $p(l_2 \rightarrow 90 | l_1 \rightarrow 90)$  is above chance and  $p(l_2 \rightarrow 0 | l_1 \rightarrow 90)$  is below chance for all values of  $R_1$  (Fig. 4b). Thus, by computing the conditional probabilities  $p(l_2 \rightarrow 0 | l_1 \rightarrow 0)$  and  $p(l_2 \rightarrow 0 | l_1 \rightarrow 90)$ , we obtain one set of observations affected by hysteresis and another not affected by it. The results in 4b show a clear segregation between the two sets of data, which are well described by two parallel linear functions. The vertical separation between the two functions is a measure of perceptual hysteresis.

Besides the effect of hysteresis we observe an effect of  $R_1$ . Both  $p(l_2 \rightarrow 0 | l_1 \rightarrow 0)$  and  $p(l_2 \rightarrow 0 | l_1 \rightarrow 90)$  decrease

as a function of  $R_1$ . Because  $R_1$  controls the perceptual organization of  $L_1$ , this effect could be summarized as follows: the higher the likelihood of a particular organization in  $L_1$  the lower is the likelihood of the same organization in  $L_2$ . Similar effects were interpreted in the literature as evidence of adaptation in multistable figures (reviewed in Hock et al. 1996). The effect of  $R_1$  on  $p(l_2 \rightarrow 0 | l_1 \rightarrow 90)$  corresponds to what Hock et al. (1996) called “adaptation to an unperceived organization of  $L_1$ ,” consistent with the notion that the visual system registers several organizations of a multistable stimulus, even though only one of them reaches awareness at a time.

The observation that the two sets of data are well described by two parallel linear functions implies that the effects of  $R_1$  and hysteresis on  $\text{logit}[p(l_2 \rightarrow 0)]$  are additive, confirming the independence of the two effects. This additivity in logit space means that the effects of these variables on  $p(l_2 \rightarrow 0)$  are multiplicative: the effect of  $R_1$  over its domain is to decrease  $p(l_2 \rightarrow 0)$  by a factor of 4.6; the effect of hysteresis increases  $p(l_2 \rightarrow 0)$  by a factor of 18.1.

## Experiment 2

In this experiment we rotated  $L_2$  with respect to  $L_1$  to find a range of angular alignment between  $L_1$  and  $L_2$  for which the correlations between the percepts of the two stimuli still hold.

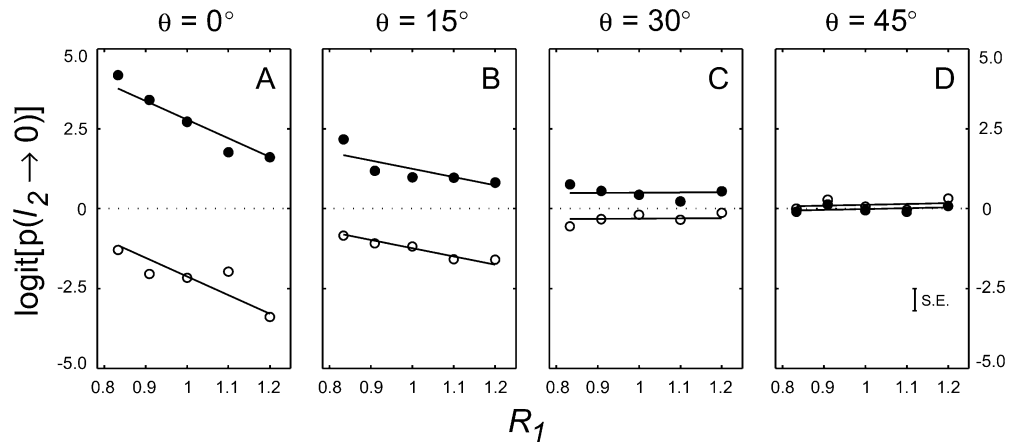
### Method

In this experiment we used square (rather than hexagonal) lattices as  $L_2$  and rotated them with respect to  $L_1$  by an angle  $\theta$  ( $0^\circ \leq \theta \leq 45^\circ$ ), in four steps of  $15^\circ$ . In square lattices, the inter-dot distances along  $0^\circ$  and  $90^\circ$  are equal and the corresponding most likely percepts are equiprobable and equally misaligned with the rectangular  $L_1$  lattice. The angle  $\theta=45^\circ$  was a control condition, in which  $l_2 \rightarrow 0$  is equidistant from the adapting orientations of  $0^\circ$  and  $90^\circ$ . The duration of  $L_1$  was 500 ms. Three observers participated in this experiment. None of the observers knew the purpose of the experiment. The experiment was otherwise identical to experiment 1.

### Results

We averaged the values of  $\text{logit}[p(l_1 \rightarrow 0)]$ , which were computed separately for each observer. The results are shown in Fig. 5. Although in this experiment we used a square lattice rather than a hexagonal one as  $L_2$ , at the misalignment of  $\theta=0^\circ$  the results are similar to what we observed in the first experiment: We find clear effects of both  $R_1$  and hysteresis on the perception of  $L_2$ . As expected, both effects disappear in the control condition of  $\theta=45^\circ$ , indicated by the lack of vertical separation between

**Fig. 5** Results of experiment 2. **a–d** Plots for the four values of orientation misalignment ( $\theta$ ) between  $L_1$  and  $L_2$ . Each plot uses the format of 4b, where  $\theta$  was equal to  $0^\circ$ .



the data sets  $p(l_2 \rightarrow 0 | l_1 \rightarrow 0)$  and  $p(l_2 \rightarrow 0 | l_1 \rightarrow 90)$ , and the lack of a negative slope in the fitting functions.

The effects of  $R_1$  and hysteresis behave differently as a function of  $\theta$ . As we increase  $\theta$ , the slopes of both functions  $p(l_2 \rightarrow 0 | l_1 \rightarrow 0)$  and  $p(l_2 \rightarrow 0 | l_1 \rightarrow 90)$  rapidly drop to zero. We summarize these results in Fig. 6 by plotting the average slope of the two functions against  $\theta$ . Evidently, the effect of  $R_1$  is substantially reduced (by a factor of 4) as  $\theta$  grows from  $0^\circ$  to as small a misalignment as  $15^\circ$ . The effect of  $R_1$  disappears completely at  $\theta=30^\circ$ . On the contrary, the effect of hysteresis is still evident at  $\theta=30^\circ$ , although it is reduced by a factor of 6 compared to its maximal value at  $\theta=0^\circ$ .

## Discussion

We presented observers with two successive dot lattices— $L_1$  and  $L_2$ —and manipulated the aspect ratio of  $L_1$ . We found two contingencies between the perception of successive stimuli: (1) observers preferred to see the same organization in  $L_1$  and  $L_2$ , but (2) increasing the likelihood of an organization in  $L_1$  decreased the likelihood of seeing the same organization in  $L_2$ , whether or not that organization was experienced in  $L_1$ .

Observers' preference for the same perceptual organization is a manifestation of perceptual persistence that is often called hysteresis. The second effect is the negative

contingency between the likelihood (strength) of a potential percept in the preceding stimulus and the likelihood of seeing the same organization in the succeeding stimulus. Similar negative contingency has been attributed to sensory adaptation (Hock et al. 1996). Adopting the above view of perceptual selection, we could summarize our results as follows. We showed that unperceived interpretations of static perceptual groupings cause selective orientation-tuned adaptation just as they do in multistable apparent motion. Beyond that, we also measured the contribution of perceptual hysteresis and found that the effects of adaptation and hysteresis are independent and combine multiplicatively.

## Hypothesis of persistent bias

Our results also agree with a different hypothesis that explains the contingencies between perception of successive multistable figures without invoking mechanisms such as hysteresis or adaptation.

Repetitive changes in the perception of unchanging multistable figures reveal a factor of perceptual organization which is intrinsic to the brain and which alters perception in an apparently random fashion (Borsellino et al. 1972; Ditzinger and Haken 1990; Hock et al. 1997; Hock et al. 2003; Hupé and Rubin 2003). We will call this factor an *intrinsic bias*. Because of this bias the perception of multistable figures is probabilistic: we know the likelihood of a particular percept but we are not certain whether the percept would occur in a particular trial. By varying stimulus geometry, however, we can change the likelihood of the percept. For example, events  $l_1 \rightarrow 0$  are more likely than events  $l_1 \rightarrow 90$  when  $R_1 > 1$ . We will call such contribution of stimulus geometry a *stimulus support* of a particular organization in a multistable figure.

Multistable figures can be perceived in a way inconsistent with stimulus support. For example, event  $l_1 \rightarrow 0$  happens with a measurable likelihood when  $R_1 < 1$ , even though stimulus support favors  $l_1 \rightarrow 90$ . Presumably, such events come about when intrinsic bias happens to exceed stimulus support. How do the fluctuations of intrinsic bias

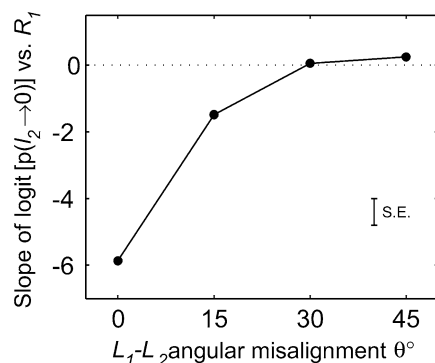


**Fig. 6** Summary of experiment 2. The negative slopes in 5 vanish as the angular misalignment  $\theta$  between  $L_1$  and  $L_2$  approaches  $30^\circ$ .

relative to stimulus support manifest themselves in our results?

Consider, first, those cases where event  $l_1 \rightarrow 0$  happened at  $R_1 \ll 1$  (Fig. 4A), i.e., against the stimulus support of  $L_1$ . In those trials, the intrinsic bias that favored  $l_1 \rightarrow 0$  was presumably greater than the stimulus support. Notice also that after event  $l_1 \rightarrow 0$  at  $R_1 \ll 1$ , we found a high likelihood of event  $l_2 \rightarrow 0$  (top left in Fig. 4b). That is to say, observers were likely to see  $L_2$  organized parallel to  $0^\circ$  after they saw  $L_1$  organized parallel to  $0^\circ$ , against the stimulus support of  $L_1$ . It seems plausible that the same intrinsic bias that overcame stimulus support in favor of  $0^\circ$  in  $L_1$  also tipped the balance in favor of  $0^\circ$  in  $L_2$ , whose geometry was equally consistent with both  $0^\circ$  and  $90^\circ$  interpretations.

When  $R_1 \gg 1$ , however, events  $l_1 \rightarrow 0$  occur in agreement with the stimulus support of  $L_1$ , so that the data in the right part of the top function in Fig. 4b do not correspond to only those trials where intrinsic bias supported  $0^\circ$ . Consistent with this observation, we found that here function  $p(l_2 \rightarrow 0 | l_1 \rightarrow 0)$  drops toward the chance level, as one would expect from the neutral configuration of  $L_2$  (recall that  $R_2=1$ ).

Thus both the elevation of the left end of function  $p(l_2 \rightarrow 0 | l_1 \rightarrow 0)$  (which we previously attributed to hysteresis) and the proximity of its right end to the chance level (which we previously attributed to adaptation) can be explained using the basic notion of intrinsic bias alone. Similarly, the low likelihood of  $l_2 \rightarrow 0$  after  $l_1 \rightarrow 90$  at  $R_1 > 1$  (the right end of the bottom function in Fig. 4b), and the closure of  $p(l_2 \rightarrow 0 | l_1 \rightarrow 90)$  to chance level at  $R_1 < 1$  can also be explained using the hypothesis of intrinsic bias alone. The only constraint that this hypothesis puts on the properties of intrinsic bias is that at the successive instants of  $L_1$  and  $L_2$  the biases must be similar. We will refer to this idea as *hypothesis of persistent bias*.

Next we test the hypothesis of persistent bias by formulating it explicitly, as a probabilistic model. In a simulation of the model below we examine whether the hypothesis of persistent bias alone can explain both effects observed in Fig. 4b.

### Model of persistent bias

We formulated the model as a sequence of trials (or iterations), each simulating successive presentations of lattices  $L_1$  and  $L_2$ . Each iteration of our simulation proceeded through the following steps:

#### Stimulus support

We computed the attraction strength  $s_i^v$  for each potential direction  $\mathbf{v}$  (where  $\mathbf{v} \in \{\mathbf{b}, \mathbf{c}, \mathbf{d}\}$ ) in the dot lattices  $L_i$  (where  $i = 1, 2$ ), using the Pure Distance Model of grouping by proximity of Kubovy et al. 1998

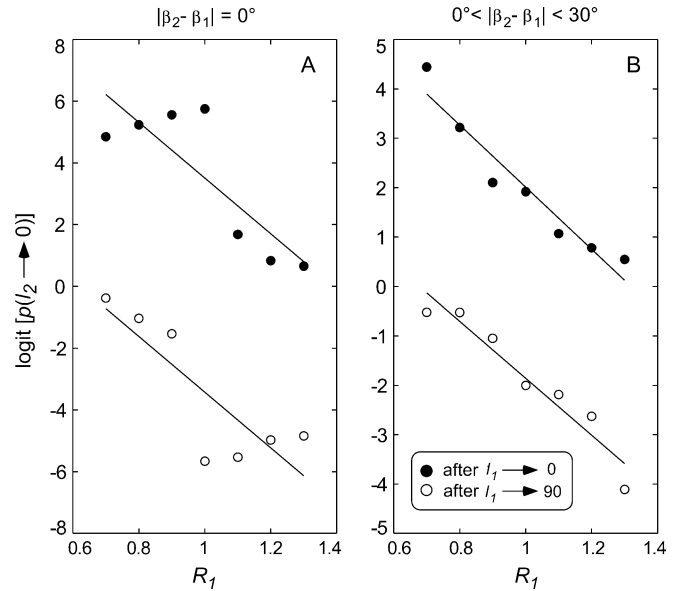


**Fig. 7** Results of a Monte Carlo simulation of the model of persistent bias with 200 iterations per condition. **a** The simulated data show a “crispening” pattern when the bias distribution does not change across time ( $\beta_1 = \beta_2$ ). **b** The simulation yields a pattern similar to the one observed in the human data (Fig. 4b) when the bias is allowed to change (Fig. 8).

$$s_i^v = e^{-\alpha \left( \frac{|\mathbf{v}|}{|\mathbf{a}|} - 1 \right)}, \quad (3)$$

where  $\alpha$  is the *attraction constant*,  $|\mathbf{v}|$  is the inter-dot distance in the direction of organization  $\mathbf{v}$ , and  $|\mathbf{a}|$  is the inter-dot distance of the organization  $L_1 \rightarrow 0$ . The Pure Distance Model describes how the attraction strength of a certain organization decays as a function of the corresponding inter-dot distance, normalized by a reference inter-dot distance  $|\mathbf{a}|$ :

$$s_i^v \begin{cases} > 1 & : & 0 < |\mathbf{v}| < |\mathbf{a}| \\ = 1 & : & |\mathbf{v}| = |\mathbf{a}| \\ < 1 & : & |\mathbf{v}| > |\mathbf{a}| \end{cases}. \quad (4)$$

The attraction constant  $\alpha$ , which typically varies across observers between 5 and 10, is an index of an observer’s sensitivity to the ratio of proximities between the alternative organizations: the larger attraction constant, the higher observer’s sensitivity. (For the simulations summarized in Fig. 7,  $\alpha=7$ .)

#### Intrinsic bias

In our model, bias is a stimulus-independent distribution supporting perceptual organizations for a range of orientations. The mean  $\beta_1$  of the bias distribution was drawn from the Uniform distribution on the circle:

$$U_c(\theta) = 2\pi U_l, \quad (5)$$

where  $U_i$  is a uniformly distributed random variable on the line interval  $[0,1]$ . The random placement of bias distribution in the beginning of every trial reflects the fact that in our experiments the conditions were randomized across trials, so that any configuration could occur before the current trial. Hence, our method allows us to study contingencies of responses within, and not between, the trials.

We simulated the bias distribution, centered on  $\beta_1$ , using the Wrapped Cauchy distribution  $W(\theta)$ ,  $0 \leq \theta < 2\pi$  (Fisher 1993, pp. 46–47), which is a computationally efficient approximation to the Gaussian distribution wrapped around the circle. The standard deviation of the distribution was  $30^\circ$ . We computed the weights  $w^v \in W(\theta)$  of the bias distribution by drawing values of  $W(\theta)$  at the corresponding orientations.

To implement the hypothesis of persistent bias, the mean  $\beta_2$  of the bias distribution during the presentation of  $L_2$  had to be similar to  $\beta_1$ . (We will explain how this was achieved in the forthcoming section, “Change of bias across time.”)

*Decision*

Compute the energy  $E_i^v$  for each of the four orientations:

$$E_i^v = s_i^v w^v \tag{6}$$

and determine which organization is perceived by choosing the orientation that has the highest energy.

*Change of bias across time*

The hypothesis of persistent bias holds that the orientation bias in the  $L_2$  phase of each iteration is identical or similar to the bias in the  $L_1$  phase. To implement this idea, we either chose  $\beta_2 = \beta_1$  or allowed  $\beta_2$  to slightly drift away from  $\beta_1$ . It turns out that this difference causes a significant change in simulation outcomes.

If  $\beta_2 = \beta_1$  (i.e., if the bias distribution does not change during the interval between  $L_1$  and  $L_2$ ) the data show a

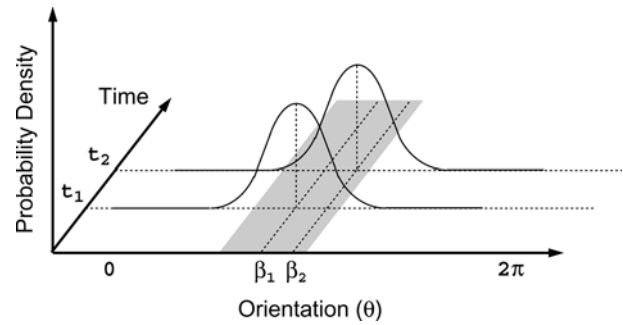


**Fig. 8** Change in the distribution of intrinsic bias across time, shown on the line rather than on the circle for simplicity. At time  $t_1$  the bias is centered on  $\beta_1$ . At time  $t_2$  it is centered on  $\beta_2$ , drawn from a uniform distribution on a narrow interval of  $\theta$  (shaded area) whose mean is  $\beta_1$ .

“crispening pattern,” evident in Fig. 7a:

$$\begin{aligned} & \text{logit}[p(l_2 \rightarrow 0 | l_1 \rightarrow 0)] \\ &= f(R_1) \begin{cases} \text{increasing} & R_1 \leq 1 \\ \text{decreasing} & R_1 > 1. \end{cases} \end{aligned} \tag{7}$$

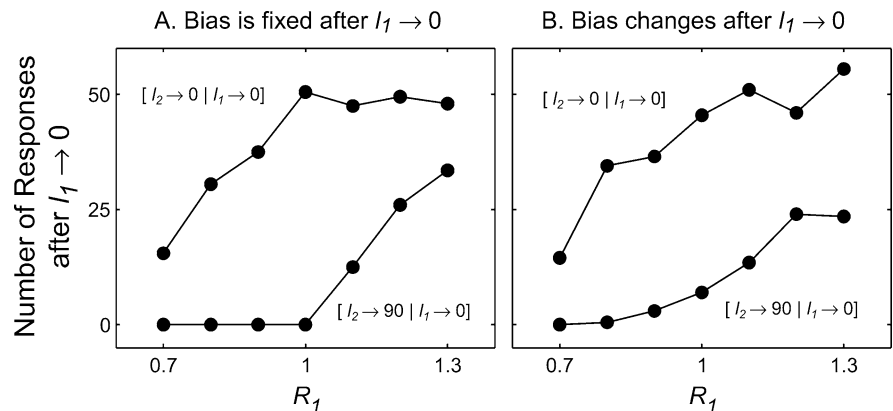
Similarly,

$$\begin{aligned} & \text{logit}[p(l_2 \rightarrow 0 | l_1 \rightarrow 90)] \\ &= f(R_1) \begin{cases} \text{increasing} & R_1 \geq 1 \\ \text{decreasing} & R_1 < 1. \end{cases} \end{aligned} \tag{8}$$

(We explain the causes of “crispening” in the next section.) When, however, the mean of the intrinsic bias distribution changes over time ( $\beta_2 \neq \beta_1$ ), the model yields results similar to human data (Fig. 7b).

In the simulation that generated the results shown in Fig. 7b, we implemented the change of bias by drawing  $\beta_2$  from a narrow uniform probability distribution  $U_b$  centered on  $\beta_1$  (Fig. 8). Except for its mean  $\beta_2$ , this distribution was identical to the one we used in the  $L_1$  phase. The results shown in Fig. 7b were obtained with the range of  $U_b$  equal to the standard deviation of the bias distribution ( $30^\circ$ ). As the range of  $U_b$  grows, the negative slopes of the two functions in Fig. 7b approach zero (not

**Fig. 9** The frequencies of events  $l_2 \rightarrow 0$  and  $l_2 \rightarrow 90$  after  $L_1$  has been organized parallel to  $0^\circ$ . **a** The bias distribution was identical in the  $L_1$  and  $L_2$  phases of each trial. **b** The bias distribution was allowed to slightly change during the interval between the  $L_1$  and  $L_2$  phases (Fig. 8). The results of simulations displayed in **a** and **b** were used to obtain the results shown with filled dots on the top of Fig. 4a and b, respectively.



shown in the figure). Increasing the range of  $U_b$  is equivalent to rotating  $L_2$  relative to  $L_1$ , because in both cases the bias tuned to  $0^\circ$  in the  $L_1$  phase of a trial will not systematically affect the organization of  $L_2$ . This observation implies that the hypothesis of persistent bias is also consistent with our findings in experiment 2, that increasing the angular misalignment of  $L_1$  and  $L_2$  brings  $L_2$  out of the effective range of the orientation-tuned bias.

### The causes of “crispening”

We found that if the simulated intrinsic bias does not change between the successive stimuli, the model yields a “crispening pattern” (Fig. 7a) that is not observed in the human data (Fig. 4b). To clarify the causes of “crispening” we plot the simulation results in the format of Fig. 9. The figure displays the number of simulated events [ $l_2 \rightarrow 0 | l_1 \rightarrow 0$ ] and [ $l_2 \rightarrow 90 | l_1 \rightarrow 0$ ]. The log-ratio between the two data sets in Fig. 9a yields the top function in Fig. 7a. This function deviates from the human data when  $R_1 \leq 1$ . Let us consider the cases of  $R_1=1$  and  $R_1 < 1$  separately.

When  $R_1=1$ , events  $l_1 \rightarrow 0$  happen only when the intrinsic bias favors organization parallel to  $0^\circ$ . Thus, when  $\beta_1=\beta_2$  (as in Fig. 9a),  $L_2$  is always organized the same way as  $L_1$ . This explains the fact that events [ $l_2 \rightarrow 90 | l_1 \rightarrow 0$ ] never occur when  $R_1=1$ . However, when  $\beta_1 \neq \beta_2$  (as in Fig. 9b), the intrinsic bias will sometimes support  $0^\circ$  and sometimes  $90^\circ$  in the  $L_1$  phase, such that  $L_2$  will also be organized sometimes parallel to  $0^\circ$  and sometimes parallel to  $90^\circ$ .

When  $R_1 \ll 1$ , the stimulus geometry in  $L_1$  does not favor organization parallel to  $0^\circ$ , so that events  $l_1 \rightarrow 0$  happen only when the intrinsic bias supports  $0^\circ$ . Thus, when  $\beta_1=\beta_2$ ,  $L_2$  can only be organized parallel to  $0^\circ$  (Fig. 9a). As  $R_1$  grows within  $R_1 < 1$ , the stimulus support against  $0^\circ$  decreases and events  $l_1 \rightarrow 0$  happen more often. When  $\beta_1 \neq \beta_2$ ,  $L_2$  can sometimes be organized parallel to  $90^\circ$  after the bias has caused organization  $0^\circ$  in  $L_1$  and has moved away such as to support organization  $90^\circ$  in  $L_2$ .

A similar analysis applies to the increasing segment of the data set [ $l_2 \rightarrow 0 | l_1 \rightarrow 90$ ] at  $R_1 \geq 1$  in Fig. 7a.

### Probability matching in perception?

What purpose could be served by having a system in which an orientation bias drifted over time? We can suggest an account by recalling the phenomenon of probability matching (also known as probability learning; e.g., Estes 1964 and Gallistel 1990, pp 351–383). It has been observed that when animals and humans are given the choice between two alternatives, one of which is rewarded more often than the other, they choose each alternative roughly in proportion to the likelihood of reward. This strategy does not maximize payoff. So why would organisms evolve to favor it? Because it is suboptimal only in a world in which probabilities are stable. If the animal assumed that the world may change

and that the resource at the most generous source is more likely to be exhausted, then the strategy according to which it chooses the most likely alternative may turn out to be shortsighted, and may fail in the long run. Similarly, there is good reason to have a perceptual system evolve in such a way that when the environment admits of more than one interpretation, one sometimes favors one, and other times another, even when one of the interpretations is more likely to be correct. Indeed, probability matching occurs in visual behavior (Kowler and Anton 1987; Triesch et al. 2002). A drifting orientation bias could be an instantiation of such a perceptual strategy.<sup>2</sup>

Perceptual multistability may be a special case of the organism’s attempt to take into account as much information as possible. Depending on whether the information from different sources is consistent or not, the organism may treat multiple source of information as being antagonistic or synergistic. When the information is consistent, all the sources contribute to the percept (for example, by taking the weighted sum of the corresponding estimates: Landy and Kojima 2001; Ernst and Banks 2002; Gepshtein and Banks 2003; Alais and Burr 2004, or by being super-additive: Kubovy et al. 1999). When it is inconsistent, synergy fails and the percept is either based on a sub-additive combination of the sources (Kubovy et al. 1999) or on one of the sources at a time (winner-take-all). Because of its probabilistic nature, the latter process is sometimes called *stochastic integration* (Ghahramani et al. 1997), similar to the aforementioned probability matching.

Multistable figures are designed such that their several interpretations are conspicuously inconsistent with one other. So, it is not surprising that the dynamics of multistability resemble that of stochastic integration. It remains to be seen whether the model of drifting bias, which we have shown to account for the dynamics of multistable figures, can also explain the dynamics of other cases of stochastic integration.

**Acknowledgements** We are grateful to H. Hock and D. R. Proffitt for valuable discussions, and to W. Epstein, H. Hock, and J. Wagemans for helpful suggestions about an early version of the manuscript.

### References

- Alais D, Burr D (2004) The ventriloquist effect results from near-optimal bimodal integration. *Curr Biol* 14:257–262
- Barlow HB (1990) A theory about the functional role and synaptic mechanism of visual after-effects. In: Blakemore C (ed) *Vision: coding and efficiency*. Academic Press, New York, pp 363–375
- Blake R, Logothetis NK (2002) Visual competition. *Nat Rev Neurosci* 3:13–21
- Borsellino A, Allazetta A, Bartolini B, Rinesi S, DeMarco A (1972) Reversal time distribution in the perception of visual ambiguous stimuli. *Kybernetik* 10:139–144

<sup>2</sup>For other views on why vision might “shake up” the organization of the input, and allow for solutions that are not favored by stimulation, see Carpenter (1999) and Leopold and Logothetis (1999).

- Carlson VR (1953) Satiation in a reversible perspective figure. *J Exp Psychol* 45:442–448
- Carpenter RHS (1999) A neural mechanism that randomises behavior. *J Consc Studies* 6:13–22
- Ditzinger T, Haken H (1990) The impact of fluctuations on the recognition of ambiguous patterns. *Biol Cybern* 63:453–456
- Ernst MO, Banks MS (2002) Humans integrate visual and haptic information in a statistically optimal fashion. *Nature* 415:429–433
- Estes WK (1964) Probability learning. In: Melton AW (ed) *Categories of human learning*. Academic Press, New York
- Fender D, Julesz B (1967) Extension of Panum's fusional area in binocularly stabilized vision. *J Opt Soc Am A* 57:819–830
- Fisher NI (1993) *Statistical analysis of circular data*. Cambridge University Press, New York
- Gallistel CR (1990) *The organization of learning*. MIT Press, Cambridge
- Gepshtein S, Banks MS (2003) Viewing geometry determines how vision and touch combine in size perception. *Curr Biol* 13:483–488
- Ghahramani Z, Wolpert DM, Jordan MI (1997) Computational models of sensorimotor integration. In: Morasso PG, Sanguineti V (eds) *Self-organization, computational maps and motor control*. Elsevier, New York, pp 117–147
- Hochberg JE (1950) Figure-ground reversal as a function of visual satiation. *J Exp Psychol* 40:682–686
- Hock HS, Kelso JAS, Schöner G (1993) Bistability and hysteresis in the organization of apparent motion patterns. *J Exp Psychol Hum Percept Perform* 19:63–80
- Hock HS, Schöner G, Giese M (2003) The dynamical foundations of motion pattern formation: stability, selective adaptation, and perceptual continuity. *Percept Psychophys* 65:429–457
- Hock HS, Schöner G, Hochstein S (1996) Perceptual stability and the selective adaptation of perceived and unperceived motion directions. *Vision Res* 36:3311–3323
- Hock HS, Schöner G, Voss A (1997) The influence of adaptation and stochastic fluctuations on spontaneous perceptual changes for bistable stimuli. *Percept Psychophys* 59:509–522
- Hupé JM, Rubin N (2003) The dynamics of bi-stable alternation in ambiguous motion displays: a fresh look at plaids. *Vision Res* 43:531–548
- Ittelson WH (1952) *The Ames demonstrations in perception*. Princeton University Press, Princeton
- Julesz B, Chang JJ (1976) Interaction between pools of binocular disparity detectors tuned to different disparities. *Biol Cybern* 22:107–119
- Kanizsa G, Luccio R (1995) Multistability as a research tool in experimental phenomenology. In: Kruse P, Stadler M (eds) *Ambiguity in mind and nature*. Springer, Berlin Heidelberg New York, pp 47–68
- Köhler W, Wallach H (1944) Figural aftereffects; an investigation of visual processes. *Proc Am Phil Soc* 88:269–357
- Kowler E, Anton S (1987) Reading twisted text—implications for the role of saccades. *Vision Res* 27:45–60
- Kruse P, Stadler M (eds) (1995). *Ambiguity in mind and nature*. Springer, Berlin Heidelberg New York
- Kruse P, Stadler M, Wehner T (1986) Direction and frequency specific processing in the perception of long-range apparent movement. *Vision Res* 26:327–335
- Kubovy M (1994) The perceptual organization of dot lattices. *Psychon Bull Rev* 1:182–190
- Kubovy M, Cohen DJ, Hollier J (1999) Feature integration that routinely occurs without focal attention. *Psychon Bull Rev* 6:183–203
- Kubovy M, Holcombe AO, Wagemans J (1998) On the lawfulness of grouping by proximity. *Cognit Psychol* 35:71–98
- Kubovy M, Wagemans J (1995) Grouping by proximity and multistability in dot lattices: a quantitative gestalt theory. *Psychol Sci* 6:225–234
- Landy MS, Kojima H (2001) Ideal cue combination for localizing texture-defined edges. *J Opt Soc Am A* 18:2307–2320
- Leopold DA, Logothetis NK (1999) Multistable phenomena: changing views in perception. *Trends Cognit Sci* 3:254–264
- Marr D (1982) *Vision*. Freeman, New York
- Rock I (1975) *Introduction to perception*. Macmillan, New York
- Triesch J, Ballard DH, Jacobs RA (2002) Fast temporal dynamics of visual cue integration. *Perception* 31:421–434
- von Helmholtz H (1867/1962). *Treatise on physiological optics*, vol III. Originally published in 1867. Dover, New York
- von Schiller P (1933) Stroboskopische Alternativversuche. *Psychol Forsch* 17:179–214
- Williams D, Phillips G, Sekuler R (1986) Hysteresis in the perception of motion direction as evidence for neural cooperativity. *Nature* 324:253–255